Published in final edited form as:
Magn Reson Imaging. 2014 September ; 32(7): 891–898. doi:10.1016/j.mri.2014.04.017.

Evaluation of Aortic Stenosis Severity using 4D Flow Jet Shear Layer Detection for the Measurement of Valve Effective Orifice Area

Julio Garcia[1,2,§], **Michael Markl**[1,3], **Susanne Schnell**[1], **Bradley Allen**[1], **Pegah Entezari**[1], **Riti Mahadevia**[1], **S Chris Malaisrie**[4], **Philippe Pibarot**[2], **James Carr**[1], and **Alex J Barker**[1]

[1]Radiology, Northwestern University, Chicago, USA

[2]Medicine, Laval University, Quebec, Canada

[3]Biomedical Engineering, Northwestern University, Chicago, USA

[4]Division of Cardiothoracic Surgery, Northwestern University, Chicago, USA

Abstract

Aims—The objective of this study was to evaluate the potential of 4D flow MRI to assess valve effective orifice area (EOA) in patients with aortic stenosis as determined by the jet shear layer detection (JSLD) method.

Methods and Results—An in-vitro stenosis phantom was used for validation and in-vivo imaging was performed in 10 healthy controls and 40 patients with aortic stenosis. EOA was calculated by the JSLD method using standard 2D phase contrast MRI (PC-MRI) and 4D flow MRI measurements ($EOA_{JSLD\text{-}2D}$ and $EOA_{JSLD\text{-}4D}$, respectively). As a reference standard, the continuity equation was used to calculate EOA (EOA_{CE}) with the 2D PC-MRI velocity field and compared to the EOA_{JSLD} measurements. The in-vitro results exhibited excellent agreement between flow theory (EOA=0.78 cm^2) and experimental measurement ($EOA_{JSLD\text{-}4D}$=0.78±0.01 cm^2) for peak velocities ranging from 0.9 to 3.7 m/s. In-vivo results showed good correlation and agreement between $EOA_{JSLD\text{-}2D}$ and EOA_{CE} (r=0.91, p<0.001; bias: −0.01±0.38cm^2; agreement limits: 0.75 to −0.77cm^2), and between $EOA_{JSLD\text{-}4D}$ and EOA_{CE} (r=0.95, p<0.001; bias: −0.09±0.26cm^2; limits: 0.43 to −0.62cm^2).

Conclusion—This study demonstrates the feasibility of measuring EOA_{JSLD} using 4D flow MRI. The technique allows for optimization of the EOA measurement position by visualizing the 3D vena contracta, and avoids potential sources of EOA_{CE} measurement variability.

[§]Address for correspondence: Julio Garcia, Department of Radiology, Northwestern University, 737 N Michigan, Suite 1600, Chicago, USA, 60611. Phone: (312) 694-7780, Fax: (312) 926-5991, julio.flores@northwestern.edu.

Disclosures
None.

Keywords

4D flow MRI; aortic stenosis; effective orifice area; jet shear layer

INTRODUCTION

Aortic valve stenosis (AS) is the most prevalent valvular heart disease and has a 2 year mortality rate of 50% among untreated symptomatic patients with severe stenosis [1]–[3]. In the case of symptomatic severe AS, the only effective treatment is aortic valve replacement [3], [4]. Assessment of AS severity is commonly performed using transthoracic echocardiography (TTE) to quantify the valve anatomic orifice area (AOA), the effective orifice area (EOA), and the aortic valve transvalvular pressure gradient (TPG) [3], [5]. In particular, the accuracy of EOA measurement is of vital importance, given its use in stratifying challenging AS cases [3], [4], [6]. For example, irrespective of symptoms or TPG, an unfavorable outcome is predicted if a valve EOA is less than 1.0 cm^2 (where EOA is the cross-sectional area of the jet vena contracta) [6]. In other words, depending on EOA size, patients may benefit from aortic valve replacement irrespective of symptoms or other quantitative measurements of severity. Unfortunately, EOA severity assessment suffers from error propagation artifacts, is often not feasible by TTE, and is discordant with TPG in up to 20–30% of patients [6]–[8]. Hence, there exists a need to robustly and non-invasively assess valve EOA. In this respect, the jet shear layer detection (JSLD) method [9], [10] has demonstrated promise for EOA assessment when TTE measurements are discordant or difficult to obtain [3], [5], [11].

Cardiac magnetic resonance imaging (MRI) has been used in several studies to assess EOA. In particular, EOA obtained by 2D phase contrast (PC) MRI and the continuity equation has shown good correlation with TTE measurements [9], [12]–[16]. However, for both imaging modalities, the calculation of EOA requires measurements that are susceptible to error such as: aorta area, left ventricular outflow tract (LVOT) area, LVOT velocity, stroke volume, and the transvalvular velocity-time integrals [3], [9], [14], [15], [17]. For this reason, error propagation is a major drawback for the use of the continuity equation regardless of imaging modality. As an alternative, we recently demonstrated that valve EOA can be determined directly with 2D PC MRI using the JSLD method [9].

Recent implementations of MRI-derived EOA have used 2D PC MRI, which relies on the accurate placement of a 2D slice to sample complex 3D post-valve flow dynamics [9], [12], [15], [16]. This technique can be problematic in cases with highly eccentric flow, such as bicuspid aortic valves, where accurate placement is not easily feasible [18]. Given that 4D flow MRI has been shown to comprehensively capture complex 3D velocity blood flow patterns in the proximal thoracic aorta [19], [20], we hypothesize that applying the JSLD method in combination with this sequence will allow for a more accurate localization of the vena contracta and thus valve EOA estimation. The objectives of this study are to: 1) apply the JSLD method for the measurement of aortic valve EOA using 4D flow MRI, and, 2) compare 4D flow MRI-derived EOA against 2D PC-MRI-derived EOA using the JSLD and continuity equation methods.

METHODS

In vitro validation

An in vitro assessment was used to characterize the feasibility of the proposed EOA method. A simple stenosis phantom ($Ø_1$ 20.4 ± 0.5 mm, stenosis $Ø_2$ 10 ± 0.5 mm, EOA = 0.78 cm^2) with a contraction coefficient = 1 (i.e. EOA/AVA, where AVA is the anatomic valve area which there it is the cross sectional area of the stenosis phantom) by the potential flow theory was filled with water and connected to a pump under constant flow conditions (Chemflo Unit, MP Pumps, Inc; Fraser MI, USA). To increase the signal-to-noise ratio (SNR), the fluid was doped with contrast agent (Magnevist®, Bayer Schering Pharma AG, Germany) at a concentration of 1.08 mmol/L [21]. 4D flow measurements were performed on a 1.5T System (Aera, Siemens AG, Erlangen, Germany). Measurement parameters were: V_{enc} = 1–4 m/s along all three velocity encoding directions, spatial resolution 1.0×1.0×1.0 mm^3, field of view (FOV) = 350×350 mm^2, flip angle = 15°, TE/TR = 2.7–3.1/5.6–5.9 ms, scan time = 10 min.

Study population

The IRB-approved, retrospective study included 50 consented participants: ten (10) healthy control subjects (4 females, mean age 39±11 years), 15 patients (6 females, mean age 58±15 years) with tricuspid AS (0.90 $cm^2 \leq EOA_{CE} \leq 3.95$ cm^2), and 25 patients (6 females, mean age 44±11 years) with mild to severe bicuspid AS (0.95 $cm^2 \leq EOA_{CE} \leq 4.56$ cm^2). Exclusion criteria were: age<21 years old, mitral valve disease diagnosed as mild or greater, and standard contraindications to MRI. Patients with mitral valve disease were excluded because mitral regurgitation may alter the estimation of stroke volume.

Cardiac magnetic resonance imaging

Imaging was performed at 1.5T and 3T using a dedicated phased-array cardiac coil (Espree, Avanto, Skyra, Siemens AG, Erlagen, Germany). Dynamic 2D cine imaging of the heart provided a comprehensive overview of the cardiac cycle including vascular morphology and valve function as previously reported [22] [24]. Through-plane 2D PC imaging was performed in the ascending aorta (Ao, downstream of the aortic annulus) as described previously [12], [15], [23]. If phase wraps occurred, the MRI acquisition was repeated using appropriate velocity encoding. 4D flow MRI was acquired in a sagittal oblique 3D volume covering the thoracic aorta using prospective ECG gating and a respiratory navigator placed on the lung-liver interface [25]. Pulse sequence parameters for 1.5T Avanto (Espree) scans included: TE/TR = 2.3–3.4/4.8–6.6 (2.7–2.8/5.3–5.4) ms; flip angle α = 7–15° (15°), 7° if no contrast; bandwidth = 446–543 (449) MHz; temporal resolution = 38.4–52.5 (42.4–43.2) ms, and the field of view was 340–400×200–300 (240–360×255–320) mm^2 with a voxel size of 1.8–2.1×1.8–2.1×2.0–2.8 (1.7–2.5×1.8–2.2×2.2–2.3) mm^3. The 3T Skyra scan parameters were: TE/TR =2.5 ms, flip angle α = 15°, bandwidth = 449 pixel/MHz, temporal resolution = 40 ms, and field of view 400×308 mm^2 with a voxel size of 2.1×2.1×2.4 mm^3. Velocity encoding was adjusted to minimize velocity aliasing (1.5–3.0 m/s) based on 2D PC MRI scout images. Velocity encoding selection resulted in varied values for TE and TR settings. Acquisition times varied from 8 to 15 min.

Image analysis

SSFP cine images were evaluated by two observers blinded to the clinical reports, and assessment included aortic valve morphology and left ventricular function. Aortic stenosis severity was graded according to international guidelines using the valve EOA and standard 2D PC MRI continuity equation [3], [15]. Regurgitation was assessed using 2D PC MRI measurements at the level of the aortic valve [23]. Aortic size was assessed at the level of the midpoint between sinotubular junction and the origin of the innominate artery in accordance with international guidelines [26]. The presence of an ascending aortic dilation was defined by a diameter > 2.2 cm/m^2 or >4.0 cm. All 4D flow MRI data were corrected for eddy currents, Maxwell terms, and velocity aliasing using a custom-made research application in Matlab (Mathworks, Natick, Ma, USA) [27].

Determination of valve effective orifice area using the continuity equation

The MRI-derived valve EOA was calculated using the continuity equation (EOA_{CE}) and velocity measurements acquired from 2D PC-MRI [12], [14] [16]:

$$EOA_{CE} = \frac{LVEDV - LVESV}{\int_0^{t\ systole} V_{Ao}\, dt} = \frac{SV_{MRI}}{VTI_{Ao}} \quad (1)$$

where SV_{MRI} is the stroke volume derived from LV short-axis by semi-automatic segmentation (LVEDV: left ventricular end-diastolic volume; LVESV: left ventricular end-systolic volume) and VTI_{Ao} is the velocity-time integral of the peak aortic flow velocity (V_{Ao}) measured downstream of the aortic valve during systole. This method has been reported to reduce EOA error estimation when using MRI [14].

Determination of valve effective orifice area using JSLD

Aortic velocity (*V*) acquired from 2D PC MRI or 4D flow MRI was used to estimate the JSLD field via the equation JSLD = $\nabla \cdot (\omega \wedge V)$, where ω is the calculated vorticity as computed by EnSight (CEI Inc, Apex, NC) [28]–[30] and ∧ represents the wedge product. In brief, the JSLD field scales the vorticity field by the velocity magnitude, thereby providing an enhanced visualization of flow jet separation from recirculating flow (for example, downstream from a stenotic aortic valve). As a result, the transvalvular flow jet shear layer and thus the position of the vena contracta cross-sectional area (i.e. valve EOA) can be identified [9]. This technique is independent of stroke volume or velocity-time integral measurements, and thereby avoids error propagation commonly experienced with the continuity equation EOA calculation [9], [31].

The calculated 4D flow JSLD field was used to visualize the 3D vena contracta structure and position. This was achieved by defining the minimum 3D JSLD cross-sectional area and peak velocity position downstream of the aortic valve. A semiautomated contour detection algorithm (level set) was used to measure the aortic valve 2D and 4D flow EOA ($EOA_{JSLD\text{-}2D}$ and $EOA_{JSLD\text{-}4D}$) along the vena contracta cross-section (Figure 1) [9]. To initialize this algorithm, the area within the JSLD field was seeded via user interaction. The exact area was finalized using the contour algorithm to detect the contour limits of the vena contracta (i.e. EOA). The level set threshold was set to 0.1 using the weighted mean area/

length energy values obtained from each JSLD region, as reported in previous studies using 2D JSLD [9], [10]. 2D cine SSFP images were co-registered with the 4D flow data to aid with visualization of anatomic valve structure and flow [18].

Inter- and intra-observer variability

Inter- and intra- observer variability for 2D and 4D flow JSLD methods were assessed using percentage absolute error and Bland-Altman analysis in a randomized subset of 15 AS patients by two blinded observers.

Statistical analyses

Results are expressed as mean ± SD. Paired 2-tailed Student's *t*-tests or one-way ANOVA was used when appropriate. The correlation and agreement between 2D and 4D EOA_{JSLD} and EOA_{CE} measurements were assessed by the use of a Pearson's correlation coefficient and Bland-Altman plots.

RESULTS

In vitro study

Figure 2A–B shows a longitudinal slice of the 3D stenosis phantom and the resulting velocity magnitudes. The 4D flow velocity data were used to compute the normalized JSLD field and Figure 2C shows that the structure of the JSLD vena contracta remains constant for the first 4–5 EOA-equivalent diameters (distal to the stenosis). Intra-voxel dephasing due to turbulence at the flow reattachment regions was observed distal to the stenosis at approximately 5 EOA-equivalent diameters. A volumetric representation of normalized JSLD is shown in Figure 2D and an axial visualization of this structure allows the direct determination of stenosis EOA (Figure 2E). Three consecutive measurements at 10 mm downstream were averaged and resulted in an $EOA_{JSLD\text{-}4D}$ of 0.78±0.01 cm^2 (Table 1). This agrees well with the theoretical EOA, which when calculated by the potential flow theory is 0.78 cm^2 [32].

In vivo study

In the 40 patients with AS, the LV mass was 140±58 g, the LV ejection fraction was 58±12 %, the aortic through-plane velocity-time integral was 50±22 cm and the stroke volume was 97±30 mL. Mild to moderate aortic regurgitation was present in 43% (n=17, regurgitation fraction = 19±16%) of the patients and mild/moderate aortic dilation in 60% (n=24) of the patients.

Examples of valve EOA for a control subject and patients with moderate and severe AS are shown in Figure 3. The correlation of $EOA_{JSLD\text{-}4D}$ to EOA_{CE} was excellent (r= 0.95, $p<0.001$, Figure 4A). Bland-Altman analysis also showed good agreement between $EOA_{JSLD\text{-}4D}$ and EOA_{CE} (mean difference=−0.09±0.26 cm^2, limits of agreement from 0.43 to −0.62 cm^2, Figure 4B). Inter-observer variability was excellent with an absolute error of 7±6 %. Intra-observer absolute error was 2±2 % and 5±5 % for observer 1 and 2, respectively (Figure 5A). The $EOA_{JSLD\text{-}2D}$ and EOA_{CE} also showed good correlation (r= 0.91, $p<0.001$, Figure 4C). Bland-Altman analysis demonstrated good agreement between

EOA_{CE} and 2D EOA_{JSLD} methods as well (mean difference=−0.01±0.38 cm^2, limits of agreement from 0.75 to −0.77 cm^2, Figure 4D). Inter-observer variability was good with an absolute error of 9±11 %. Intra-observer absolute error was 4±3 % and 7±9 % for observer 1 and 2, respectively (Figure 5B). All EOA_{JSLD} measurements required less than 1 min for visualization, positioning, and detection using home-customized tools.

An ANOVA analysis and Tukey's range test for healthy controls and patient stenosis groups (mild, moderate, and severe AS) (Figure 6A) revealed significant differences between EOA_{CE} measurements ($p<0.05$). When using $EOA_{JSLD\text{-}4D}$, a significant difference ($p<0.001$) was found for healthy controls, patients with mild and moderate AS. The EOA estimated by the $EOA_{JSLD\text{-}4D}$ and EOA_{CE} methods was compared in each of the following 4 subsets of patients: 1. Control; 2. Presence of valve regurgitation; 3. Presence of aortic dilation (aortic diameter > 4cm); 4. Presence of valve regurgitation and aortic dilation. All patients in groups 2–4 have at least mild AS. An ANOVA test demonstrated a significant difference between groups using both CE and JSLD methods ($p<0.001$). Tukey's range test revealed a significant difference between healthy controls (group 1) and patients with aortic dilation (group 3, Figure 6B) using EOA_{CE} measurements ($p<0.05$). When $EOA_{JSLD\text{-}4D}$ measurements were used, a significant difference ($p<0.001$) was found between healthy controls (group 1), patients with aortic regurgitation (group 2), and patients with aortic dilation (group 3). A summary of EOA methods measurements is presented in table 2.

DISCUSSION

The main findings of this study were: 1) using the 4D flow technique, valve EOA_{JSLD} can be feasibly and robustly obtained in AS patients; 2) 2D and 4D flow EOA_{JSLD} correlate and agree well with the standard continuity equation method for estimation of EOA; 3) 4D flow JSLD, especially when co-registered with cine 2D SSFP images, allows for the conceptual visualization of the relationship between valve structure, 4D flow data, and the 3D structure of vena contracta, especially in cases with challenging hemodynamic conditions (such as eccentric flow jets). These findings highlight the main advantages of the $EOA_{JSLD\text{-}4D}$ method over the standard continuity equation, namely, the EOA can be directly visualized regardless of transvalvular flow jet eccentricity, and EOA calculation does not require SV and VTI measurements. This lack of dependence on SV and VTI can potentially reduce the chance for EOA measurement error and image time processing when using the $EOA_{JSLD\text{-}4D}$ method. TTE is the most frequently used imaging technique to assess AS severity, and often determines therapeutic management in clinical practice [3], [4]. However, TTE measurements are limited by reproducibility, often leading to discordant results or inadequate grading of AS severity [7], [15], [17]. In particular, the LVOT diameter measurement can significantly alter valve EOA estimation using the continuity equation [17]. In such cases, other more invasive imaging techniques such as transeophageal echocardiography, 3D echocardiography or cardiac catheterization are used to confirm AS severity.

AS severity assessment is especially important in elderly patients who exhibit a high incidence of low TPG and/or severe AS despite normal ejection fraction. However, the calculation of EOA_{CE} in these subjects is challenging, leading to referral for stress exams

(using projected valve EOA) or alternative imaging modalities to determine AS severity via valve EOA measurement [11], [33]. Additionally, the lack of reliable quantitative severity assessments often leads to a “wait for symptoms” strategy to determine if the patient will undergo aortic valve replacement, but this delay may compromise LV function recovery and patient survival [34], [35]. Consequently, risk stratification and treatment of asymptomatic patients with low TPG and low flow is a difficult challenge [11], [33], [36]. Moreover, a recent study demonstrated that valve EOA<1.0 cm^2 predicts unfavorable patient outcomes, irrespective of symptoms or TPG [6]. With these results in mind, the difference between EOA and AOA becomes important: EOA is usually smaller than AOA in patients with moderate and severe AS (Figure 3A) with both parameters physically related to each other by the valve inflow shape (Figure 3A) [32]. AOA can be assessed clinically using aortic valve planimetry, however, it can be difficult to measure AOA in heavily calcified valves and it has been shown less sensitive for predicting outcome [23], [37]. Thus, the EOA method proposed in this study may prove useful for improved risk stratification given that the technique extracts the EOA from the 3D velocity field, bypasses the reliance on additional measurements, and complements the multifactorial management of AS patients.

In this study, tricuspid and bicuspid AS patients were evaluated using 2D and 4D flow velocity measurements to compute the EOA_{JSLD} and assess AS severity. Quantification of SV in AS patients with severe aortic regurgitation is susceptible to error when using LV volumetric measurements, which will propagate and result in inaccurate EOA estimation. This difficulty may be the reason for the differences in the AR patients in Figure 6B and highlights an advantage of the JSLD method. In addition, bicuspid AS patients often present with eccentric transvalvular flow jet patterns and/or ascending aorta dilation [18]. In these scenarios, the 2D PC MRI-derived valve EOA may be overestimated due to an inadequate localization (angle or distance from the valve) of the vena contracta, and it may lead to an underestimation of velocity-time integral and TPG as calculated by the Bernoulli equation (Figure 6B) [9], [38]. In this case, Doppler echo-derived calculations will also be susceptible to errors because it is challenging to accurately position the probe to capture the eccentric jet angle for velocity assessment.

The $EOA_{JSLD\text{-}4D}$ method offers a technique that is much less dependent on plane position, systolic jet angle and flow characteristics compared with 2D phase-contrast MRI methods for EOA calculation. The inherent flexibility of the 4D flow technique is a possible reason better correlation and agreement were found between $EOA_{JSLD\text{-}4D}$ and EOA_{CE} as compared to $EOA_{JSLD\text{-}2D}$ measurements (Figure 4). Furthermore, operator and observer variability was reduced in the $EOA_{JSLD\text{-}4D}$ (Figure 5) indicating that the methodology has the potential to provide a consistent, repeatable measure of EOA.

Additional promising applications for the JSLD method include the evaluation of aortic valve kinematics by computing the instantaneous valve EOA, a measurement that has recently been performed by computing the continuity equation at all-time points in the cardiac cycle [16]. Using this technique, aortic valve kinematics have been associated with plasma levels of BNP and risk scores for asymptomatic AS patients (as recently proposed by Monin et al) [16], [39], [40]. Furthermore, the 4D flow JSLD method may also be used to evaluate the EOA of aortic valve implants (bioprosthetic and transcatheter valves), thus

improving post-operative functional assessment and possibly helping guide device development.

Study Limitations

The main limitation of this study is the small number of patients with severe AS (n=6), which is a group that would benefit the most from timely diagnosis. However, the technique was successful at identifying the severe AS patients that were included, as well as appropriately classifying patients with less severe disease. Additionally, accurate estimation of valve vorticity magnitude is dependent on the temporal and spatial resolution of the MRI scan (typically 40–50 ms per time-frame and 2–2.5 mm, respectively), which is impacts the total scan time and SNR. An adequate selection of encoded velocity or the use of unwrapping algorithms may avoid measurement errors. A general limitation of 4D flow MRI is the relatively long scan time (t=8–15 min for full aortic coverage) and data processing times (t = 20–30 min). Faster acquisition flow sequences and hardware (i.e. k-space trajectories and parallel imaging) are currently in development, and improved post-processing workflow is an active area of interest[41]. Finally, the 4D flow MRI-derived valve EOA method proposed in this study was not validated against TTE as a reliable non-invasive method to grade AS; however, the 2D JSLD method has previously shown good agreement with TTE measurements[9]. It is important to mention that, at present, there is no gold standard technique or method for the measurement of valve EOA [42]. Further studies with larger number of patients with severe stenosis are necessary to confirm the incremental diagnostic and prognostic value of this new MRI method for the valve EOA measurement.

Conclusions

The current study of aortic valve EOA calculation using the 4D flow JSLD technique demonstrates the feasibility of this method in patients with aortic stenosis. Results were compared with previously validated 2D flow-derived EOA methods and demonstrated excellent agreement. The 4D flow JSLD method may be useful to non-invasively assess AS severity without requiring the measurement of stroke volume and the transvalvular velocity-time integral. This advantage, in combination with the ability to locate the true vena contracta position, may minimize potential sources of measurement error and variability when computing valve EOA, and could ultimately lead to a larger role for EOA assessment in risk stratification and treatment planning in patients with AS. In summary, the advantages of this technique must be considered in balance with the fact that the exam time will be longer than traditional 2D methods. Thus, the proposed method targets a select AS population who exhibit discordant hemodynamic measurements with echo-Doppler and may benefit from a comprehensive flow assessment using 4D flow MRI.

Acknowledgments

This work was supported by NIH R01HL115828, AHA 13SDG14360004 grants and NUCATS Dixon Award. J. Garcia was supported by CONACyT (203355), AHA 14POST18350019 and ACCEM Laval University doctoral fellow award. Dr. Schnell is supported by the SIR Pilot Study grant and a DFG scholarship (SCHN 1170/1-1). Dr. Pibarot holds the Canada Research Chair in Valvular Heart Diseases, Canadian Institutes of Health Research, Ottawa, Ontario, Canada.

References

1. Pellikka PA, Sarano ME, Nishimura RA, Malouf JF, Bailey KR, Scott CG, Barnes ME, Tajik AJ. Outcome of 622 adults with asymptomatic, hemodynamically significant aortic stenosis during prolonged follow-up. Circulation. 2005; 111(24):3290–5. [PubMed: 15956131]
2. Carabello BA, Paulus WJ. Aortic stenosis. Lancet. 2009; 373(9667):956–66. [PubMed: 19232707]
3. Bonow RO, Carabello BA, Chatterjee K, de Leon AC, Faxon DP, Freed MD, Gaasch WH, Lytle BW, Nishimura RA, O'Gara PT, O'Rourke RA, Otto CM, Shah PM, Shanewise JS. 2008 Focused update incorporated into the ACC/AHA 2006 guidelines for the management of patients with valvular heart disease: a report of the American College of Cardiology/American Heart Association Task Force on Practice Guidelines (Writing Committee to. Circulation. 2008; 118(15):e523–661. [PubMed: 18820172]
4. Vahanian A, Alfieri O, Andreotti F, Antunes MJ, Barón-Esquivias G, Baumgartner H, Borger MA, Carrel TP, De Bonis M, Evangelista A, Falk V, Iung B, Lancellotti P, Pierard L, Price S, Schäfers HJ, Schuler G, Stepinska J, Swedberg K, Takkenberg J, Von Oppell UO, Windecker S, Zamorano JL, Zembala M. Guidelines on the management of valvular heart disease (version 2012). Eur Heart J. 2012; 33(19):2451–96. [PubMed: 22922415]
5. Pibarot P, Dumesnil JG. Improving assessment of aortic stenosis. J Am Coll Cardiol. 2012; 60(3): 169–80. [PubMed: 22789881]
6. Malouf J, Le Tourneau T, Pellikka P, Sundt TM, Scott C, Schaff HV, Enriquez-Sarano M. Aortic valve stenosis in community medical practice: Determinants of outcome and implications for aortic valve replacement. J Thorac Cardiovasc Surg. 2012; 144(6):1421–7. [PubMed: 22336754]
7. Minners J, Allgeier M, Gohlke-Baerwolf C, Kienzle RP, Neumann FJ, Jander N. Inconsistent grading of aortic valve stenosis by current guidelines: haemodynamic studies in patients with apparently normal left ventricular function. Heart. 2010; 96(18):1463–8. [PubMed: 20813727]
8. Hachicha Z, Dumesnil JG, Bogaty P, Pibarot P. Paradoxical low-flow, low-gradient severe aortic stenosis despite preserved ejection fraction is associated with higher afterload and reduced survival. Circulation. 2007; 115(22):2856–64. [PubMed: 17533183]
9. Garcia J, Marrufo OR, Rodriguez AO, Larose E, Pibarot P, Kadem L. Cardiovascular magnetic resonance evaluation of aortic stenosis severity using single plane measurement of effective orifice area. J Cardiovasc Magn Reson. 2012; 14(1):23. [PubMed: 22480269]
10. Garcia J, Capoulade R, Le Ven F, Gaillard E, Kadem L, Pibarot P, Larose E. Discrepancies between cardiovascular magnetic resonance and Doppler echocardiography in the measurement of transvalvular gradient in aortic stenosis: the effect of flow vorticity. J Cardiovasc Magn Reson. 2013; 15(1):84. [PubMed: 24053194]
11. Tandon A, Grayburn PA. Imaging of Low-Gradient Severe Aortic Stenosis. JACC Cardiovasc Imaging. 2013; 6(2):184–195. [PubMed: 23489532]
12. Caruthers SD, Lin SJ, Brown P, Watkins MP, Williams TA, Lehr KA, Wickline SA. Practical value of cardiac magnetic resonance imaging for clinical quantification of aortic valve stenosis: comparison with echocardiography. Circulation. 2003; 108(18):2236–43. [PubMed: 14568899]
13. Haghi D, Suselbeck T, Fluechter S, Kalmar G, Schroder M, Kaden JJ, Poerner T, Borggrefe M, Papavassiliu T. A hybrid approach for quantification of aortic valve stenosis using cardiac magnetic resonance imaging and echocardiography: comparison to right heart catheterization and standard echocardiography. Clin Res Cardiol. 2006; 95(3):162–7. [PubMed: 16598529]
14. Yap SC, van Geuns RJ, Meijboom FJ, Kirschbaum SW, McGhie JS, Simoons ML, Kilner PJ, Roos-Hesselink JW. A simplified continuity equation approach to the quantification of stenotic bicuspid aortic valves using velocity-encoded cardiovascular magnetic resonance. J Cardiovasc Magn Reson. 2007; 9(6):899–906. [PubMed: 18066750]
15. Garcia J, Kadem L, Larose E, Clavel MA, Pibarot P. Comparison between Cardiovascular Magnetic Resonance and Transthoracic Doppler Echocardiography for the Estimation of Effective Orifice Area in Aortic Stenosis. J Cardiovasc Magn Reson. 2011; 13(1):25. [PubMed: 21527021]
16. Garcia J, Pibarot P, Capoulade R, Le Ven F, Kadem L, Larose E. Usefulness of cardiovascular magnetic resonance imaging for the evaluation of valve opening and closing kinetics in aortic stenosis. Eur Heart J Cardiovasc Imaging. 2013; 14:819–826. [PubMed: 23299400]

17. Michelena HI, Margaryan E, Miller FA, Eleid M, Maalouf J, Suri R, Messika-Zeitoun D, Pellikka PA, Enriquez-Sarano M. Inconsistent echocardiographic grading of aortic stenosis: is the left ventricular outflow tract important? Heart. 2013; 99(13):921–31. [PubMed: 23349350]
18. Barker AJ, Markl M, Bürk J, Lorenz R, Bock J, Bauer S, Schulz-Menger J, von Knobelsdorff-Brenkenhoff F. Bicuspid aortic valve is associated with altered wall shear stress in the ascending aorta. Circ Cardiovasc Imaging. 2012; 5(4):457–66. [PubMed: 22730420]
19. Markl M, Chan FP, Alley MT, Wedding KL, Draney MT, Elkins CJ, Parker DW, Wicker R, Taylor CA, Herfkens RJ, Pelc NJ. Time-resolved three-dimensional phase-contrast MRI. J Magn Reson Imaging. 2003; 17(4):499–506. [PubMed: 12655592]
20. Meierhofer C, Schneider EP, Lyko C, Hutter A, Martinoff S, Markl M, Hager A, Hess J, Stern H, Fratz S. Wall shear stress and flow patterns in the ascending aorta in patients with bicuspid aortic valves differ significantly from tricuspid aortic valves: a prospective study. Eur Heart J Cardiovasc Imaging. 2013; 14(8):797–804. [PubMed: 23230276]
21. Lorenz R, Benk C, Bock J, Stalder AF, Korvink JG, Henning J, Markl M. Clored circuit MR compatible pulsatile pump system using a ventricular assist device and pressure control unit. Magn Reson Med. 2012; 67(1):258–68. [PubMed: 21630351]
22. Friedrich M, Schulzmenger J, Poetsch T, Pilz B, Uhlich F, Dietz R. Quantification of valvular aortic stenosis by magnetic resonance imaging. Am Heart J. 2002; 144(2):329–334. [PubMed: 12177653]
23. Cawley PJ, Maki JH, Otto CM. Cardiovascular magnetic resonance imaging for valvular heart disease: technique and validation. Circulation. 2009; 119(3):468–78. [PubMed: 19171869]
24. von Knobelsdorff-Brenkenhoff F, Rudolph A, Wassmuth R, Bohl S, Buschmann EE, Abdel-Aty H, Dietz R, Schulz-Menger J. Feasibility of cardiovascular magnetic resonance to assess the orifice area of aortic bioprostheses. Circ Cardiovasc Imaging. 2009; 2(5):397–404. [PubMed: 19808628]
25. Markl M, Harloff A, Bley TA, Zaitsev M, Jung B, Weigang E, Langer M, Hennig J, Frydrychowicz A. Time-resolved 3D MR velocity mapping at 3T: improved navigator-gated assessment of vascular anatomy and blood flow. J Magn Reson Imaging. 2007; 25(4):824–31. [PubMed: 17345635]
26. Hiratzka LF, Bakris GL, Beckman JA, Bersin RM, Carr VF, Casey DE, Eagle KA, Hermann LK, Isselbacher EM, Kazerooni EA, Kouchoukos NT, Lytle BW, Milewicz DM, Reich DL, Sen S, Shinn JA, Svensson LG, Williams DM. 2010 ACCF/AHA/AATS/ACR/ASA/SCA/SCAI/SIR/STS/SVM Guidelines for the diagnosis and management of patients with thoracic aortic disease. A Report of the American College of Cardiology Foundation/American Heart Association Task Force on Practice Guidelines. J Am Coll Cardiol. 2010; 55(14):e27–e129. [PubMed: 20359588]
27. Bock, J.; Kreher, BW.; Hennin, J.; Markl, M. Optimized pre-processing of time-resolved 2D and 3D phase contrast MRI data. 15th Scientific Meeting International Society for Magnetic Resonance in Medicine; Berlin. 2007. p. 3138
28. Garcia J, Larose E, Pibarot P, Kadem L. On the evaluation of vorticity using cardiovascular magnetic resonance velocity measurements. J Biomech Eng. 2013; 135(12):124501–6. [PubMed: 24026138]
29. Sujudi, D.; Haimes, R. Identification of swirling flow in 3D vector fields. 1995. AIAA-95-1715
30. Garcia J, Barker AJ, Schnell S, Entezari P, Mahadevia R, Pibarot P, Carr JC, Markl M. 4D Flow Jet Shear Layer Detection Method for the Measurement of Effective Orifice Area and Assessment of Aortic Stenosis Severity. J Cardiovasc Magn Reson. 2013; 15(Suppl 1):241.
31. Kadem L, Rieu R, Dumesnil JG, Durand LG, Pibarot P. Flow-dependent changes in Doppler-derived aortic valve effective orifice area are real and not due to artifact. J Am Coll Cardiol. 2006; 47(1):131–7. [PubMed: 16386676]
32. Garcia D, Pibarot P, Landry C, Allard A, Chayer B, Dumesnil JG, Durand L. Estimation of aortic valve effective orifice area by Doppler echocardiography: effects of valve inflow shape and flow rate. J Am Soc Echocardiogr. 2004; 17(7):756–65. [PubMed: 15220901]
33. Pibarot P, Dumesnil JG. Low-Flow, Low-Gradient Aortic Stenosis With Normal and Depressed Left Ventricular Ejection Fraction. J Am Coll Cardiol. 2012; 60(19):1845–53. [PubMed: 23062546]

34. Shah PK. Severe aortic stenosis should not be operated on before symptom onset. Circulation. 2012; 126(1):118–25. [PubMed: 22753533]
35. Carabello BA. Aortic valve replacement should be operated on before symptom onset. Circulation. 2012; 126(1):112–7. [PubMed: 22753532]
36. Dumesnil JG, Pibarot P, Carabello B. Paradoxical low flow and/or low gradient severe aortic stenosis despite preserved left ventricular ejection fraction: implications for diagnosis and treatment. Eur Heart J. 2010; 31(3):281–9. [PubMed: 19737801]
37. Pibarot P, Larose E. What our eyes see is not necessarily what our heart feels. Cardiology. 2008; 109(2):122–5. [PubMed: 17713327]
38. Lotz J, Meier C, Leppert A, Galanski M. Cardiovascular flow measurement with phase-contrast MR imaging: basic facts and implementation. Radiographics. 2002; 22(3):651–71. [PubMed: 12006694]
39. Garcia, J.; Capoulade, R.; Kadem, L.; Larose, É.; Pibarot, P. Valve opening and closing kinematic assessment in patients with aortic stenosis. 21st Scientific Meeting International Society for Magnetic Resonance in Medicine; Melbourne. 2013. p. 1328
40. Monin JL, Lancellotti P, Monchi M, Lim P, Weiss E, Piérard L, Guéret P. Risk Score for Predicting Outcome in Patients With Asymptomatic Aortic Stenosis. Circulation. 2009; 120:69–75. [PubMed: 19546391]
41. Schnell S, Entezari P, Mahadevia RJ, Rinewalt D, Fluckiger J, Collins J, Carr J, Jung BA, Markl M. 4D flow MRI of the aorta becomes practical : performance and observer variability for a new semi-automated workflow for 3D visualization and quantification of aortic hemodynamics. J Cardiovasc Magn Reson. 2013; 15(Suppl 1):M2.
42. Omran H, Schmidt H, Hackenbroch M, Illien S, Bernhardt P, Von Der Recke G, Fimmers R, Flacke S, Layer G, Pohl C, Luderitz B, Schild H, Sommer T. Silent and apparent cerebral embolism after retrograde catheterisation of the aortic valve in valvular stenosis : a prospective, randomised study. Lancet. 2003; 361:1241–46. [PubMed: 12699950]

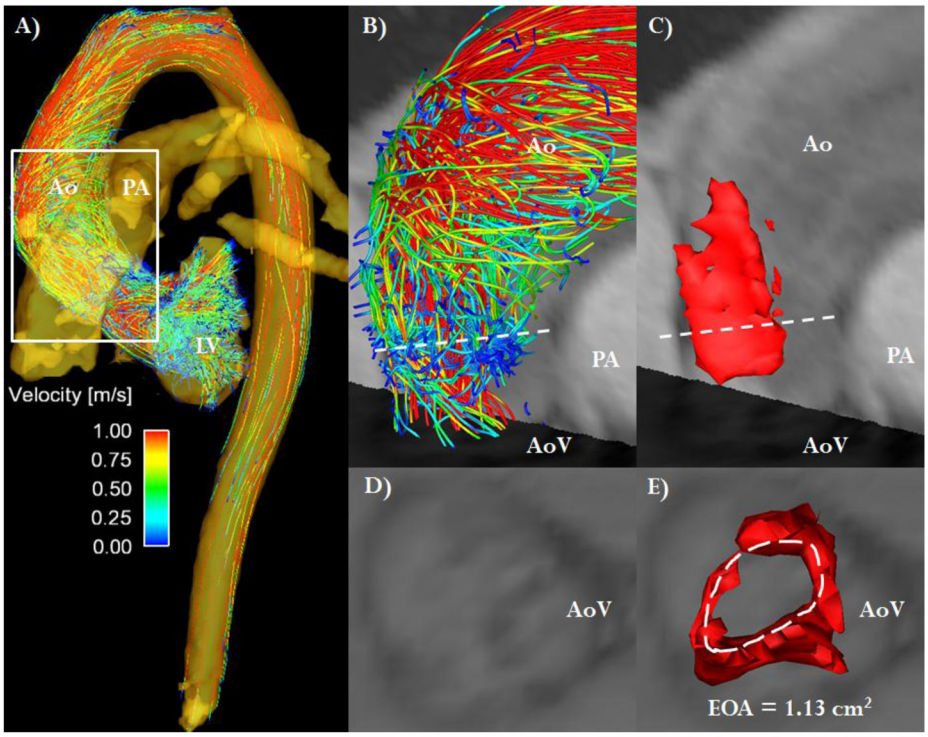

FIGURE 1. 4D flow jet shear layer detection method

Panel A shows the 3D visualization of aortic flow based on streamlines at peak systole. The white box defines the region of interest for the evaluation of aortic valve stenosis severity. Panel B shows the region of interest with the dashed white line indicating the vena contracta location. Panel C shows the same lateral 3D view of the jet shear layer detection structure used to estimate valve effective orifice area ($EOA_{JSLD-4D}$). Panel D shows the visualization of valve anatomic opening. Panel E shows the direct visualization and measurement of valve EOA by JSLD method, the dashed white line defines the vena contracta surface (i.e. EOA). Ao: Aorta, AoV: Aortic valve, LV: Left ventricle, PA: Pulmonary artery.

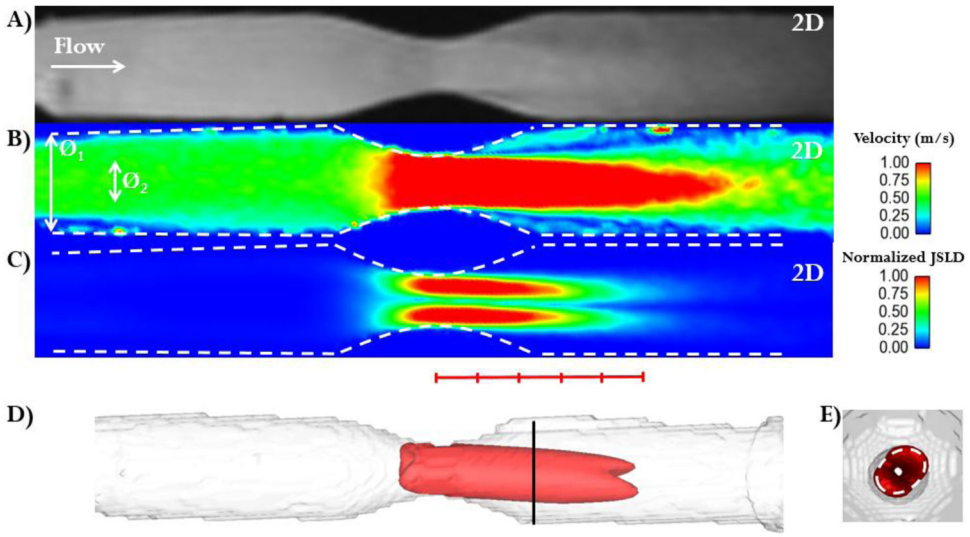

FIGURE 2. In vitro validation

Panel A: Magnitude image along the stenosis phantom z-axis. The white arrow indicates the primary flow direction. Panel B: Absolute velocity plane (in m/s) along the stenosis phantom z-axis. The white arrows indicates the phantom diameters ($Ø_1$ = 20.4 ± 0.5 mm, stenosis $Ø_2$ = 10 ± 0.5 mm). Panel C: normalized jet shear layer detection (JSLD) along the z-axis of the stenosis phantom. Panel D: 3D structure along the JSLD z-axis which was used to estimate the effective orifice area (EOA). A red line is marked with hash marks to indicate stenosis diameter. Panel E: Axial view of the 3D JSLD structure: the cross-sectional area (white dashed line) corresponds to EOA determined by the JSLD method. The oval orifice shape detected by the JSLD method matched the oval orifice geometry produced during manufacturing with a rapid prototyping printer.

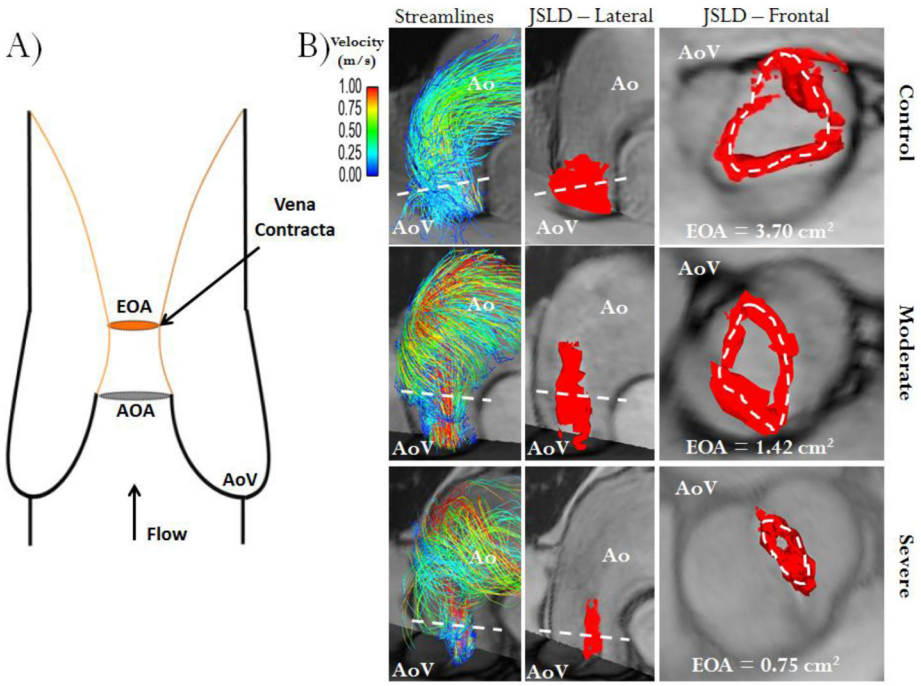

FIGURE 3. Schematic of valve effective orifice area estimation

Panel A shows an idealized representation of transaortic valve flow separation. AOA is the anatomic orifice area and EOA is the valve effective orifice area at the vena contracta (smaller area of transvalvular flow reattachment, orange lines, and maximal velocity position), note AOA>EOA. Panel B shows three different cases (control, moderate and severe aortic stenosis) using valve area estimation with the 4D flow jet shear layer detection (JSLD) method. The first column illustrates the aortic flow velocity streamlines at peak systole; the second column shows a 3D lateral view of the JSLD structure, with the red iso-surface, computed from 4D flow MRI data at peak systole; the third column shows a 3D frontal view of JSLD at peak systole. The dashed white line indicates transvalvular maximal velocity position, i.e. the vena contracta. Ao: Aorta, AoV: Aortic valve.

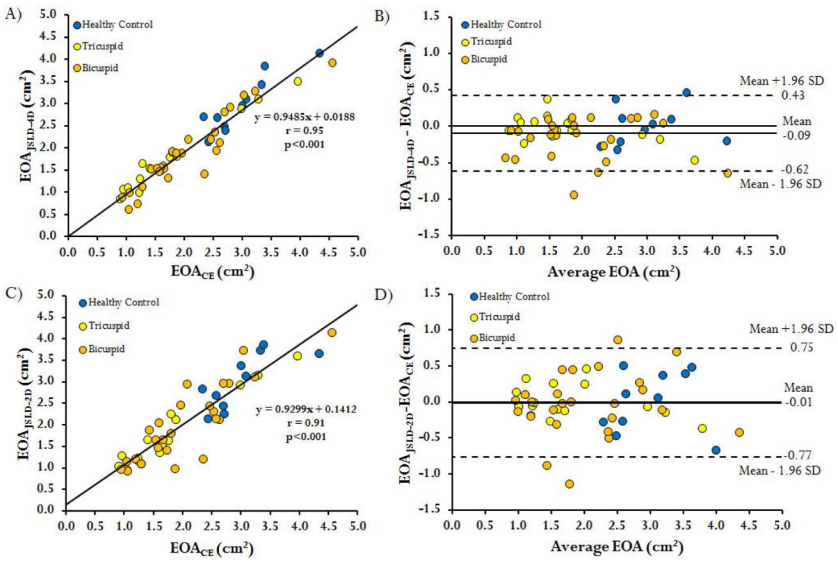

FIGURE 4. Regression and Bland-Altman plots of valve effective orifice area measurement methods

Panel A shows the regression fit of the valve effective orifice area (EOA) measured by the continuity equation using 2D PC MRI (EOA_{CE}) and the 4D flow MRI EOA measured by the jet shear layer detection method ($EOA_{JSLD\text{-}4D}$). Panel B shows the corresponding Bland-Altman agreement plot for both methods. Panel C shows the regression fit of the valve EOA measured by 2D PC MRI jet shear layer detection method ($EOA_{JSLD\text{-}2D}$) and the EOA_{CE}. Panel D shows the corresponding Bland-Altman agreement plot for both methods.

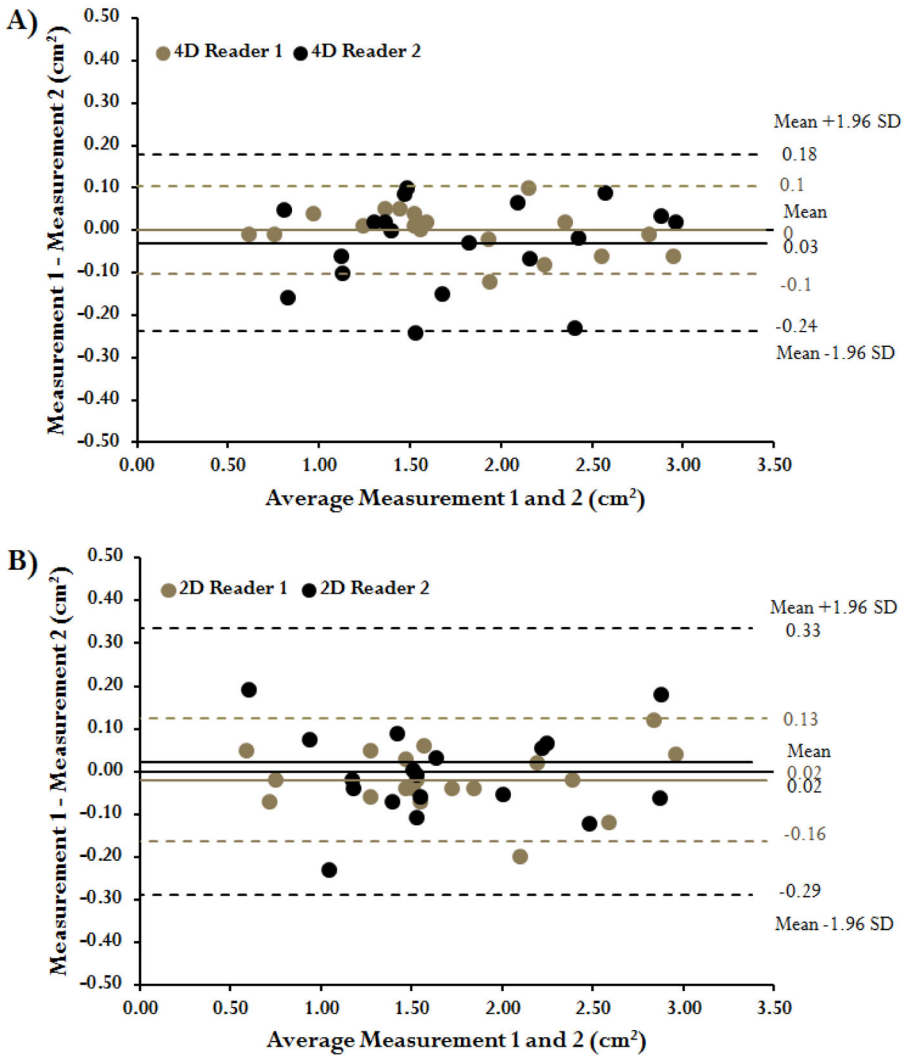

FIGURE 5. Inter-observer measurements using the 2D flow and 4D flow jet shear layer detection method

Panel A shows the Bland-Altman agreement plot for measurements performed using the 4D flow jet shear layer detection method using two blinded readers in a randomized subset of 15 patients. Panel B shows the Bland-Altman agreement plot for measurements performed using the 2D jet shear layer detection method using two blinded readers in the same subset of patients.

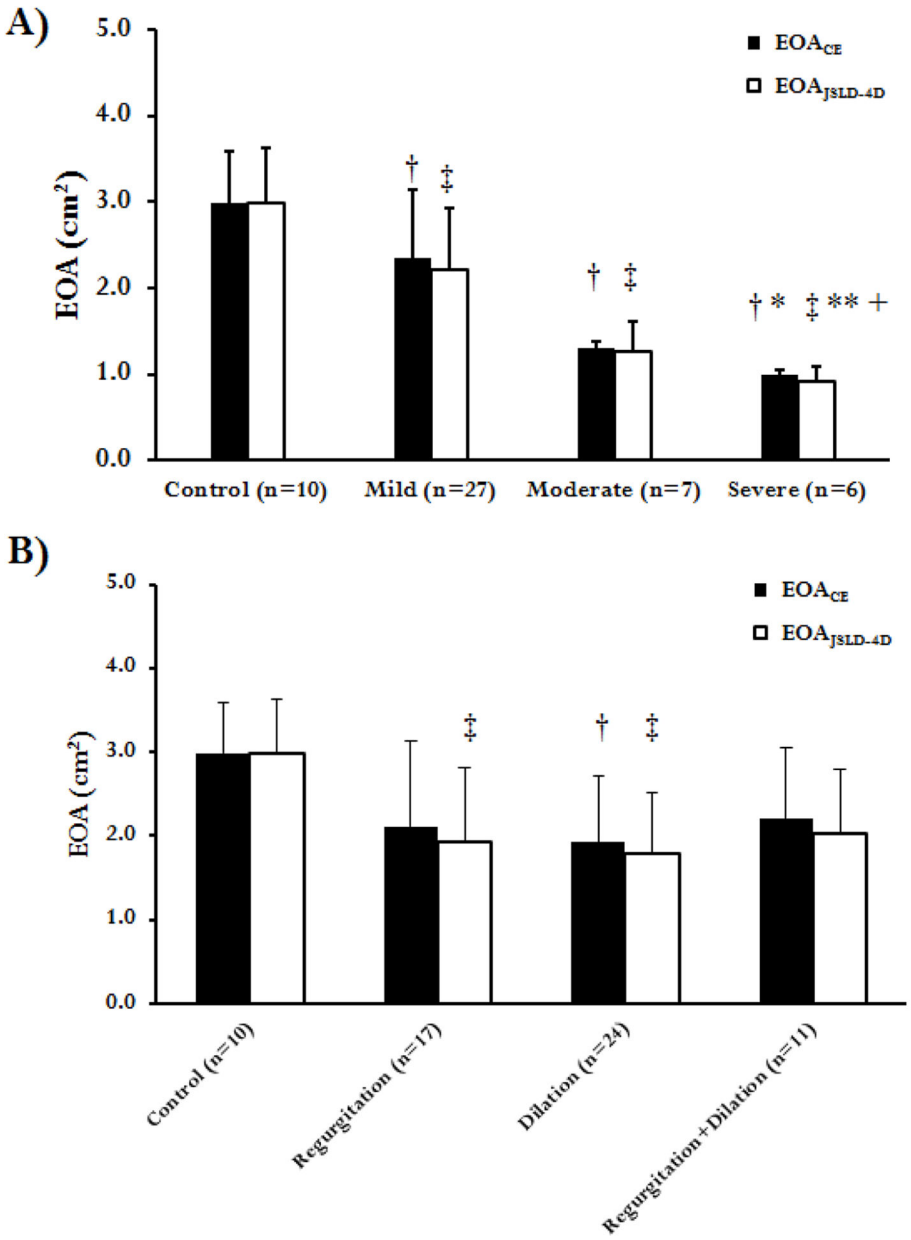

FIGURE 6. Comparison of effective orifice area using 2D PC MRI continuity equation and 4D flow jet shear layer detection method

In Panel A four subject groups (control, mild, moderate and severe aortic stenosis) were compared by an ANOVA test. In Panel B four subjects groups (control, aortic valve regurgitation, aortic aneurysm, combined valve regurgitation and aortic aneurysm) were compared by an ANOVA test. †: $p<0.05$ or ‡: $p<0.001$ as compared to controls; *: $p<0.05$ or **: $p<0.001$ as compared to mild AS; +: $p<0.001$ as compared to moderate AS.

Table 1

Summary of in-vitro measurements.

Peak Velocity (m/s)	Theoretical EOA (cm^2)	EOA_{CE} (cm^2)	$EOA_{JSLD-2D}$ (cm^2)	$EOA_{JSLD-4D}$ (cm^2)
0.9	0.78	0.75	0.75 ± 0.02	0.77 ± 0.01
1.8	0.78	0.78	0.81 ± 0.03	0.78 ± 0.02
2.8	0.78	0.79	0.77 ± 0.03	0.78 ± 0.01
3.7	0.78	0.81	0.81 ± 0.03	0.77 ± 0.02

Theoretical effective orifice area (EOA) was calculated by the potential flow theory. EOA by continuity equation (EOA_{CE}) was computed used a simplified version given by $EOA_{CE}=SV/Vmax$. EOA by jet shear layer detection method was calculated in 2D ($EOA_{JSLD-2D}$) and 4D ($EOA_{JSLD-4D}$) using the calculated JSLD field.

Table 2

Summary of EOA measurements in evaluated subjects.

	EOA_{CE} (cm^2)	$EOA_{JSLD-2D}$ (cm^2)	$EOA_{JSLD-4D}$ (cm^2)
Controls (n=10)	2.98 ± 0.59	3.01 ± 0.63	2.98 ± 0.64
Patients (n=40)	1.96 ± 0.85	1.94 ± 0.86	1.81 ± 0.81